Influence of hummocks and emergent vegetation on hydraulic performance in a surface flow wastewater treatment wetland

Steffanie H. Keefe,[1] Joan S. (Thullen) Daniels,[2] Robert L. Runkel,[2] Roland D. Wass,[3] Eric A. Stiles,[4] and Larry B. Barber[1]

Received 5 May 2010; accepted 27 July 2010; published 11 November 2010.

[1] A series of tracer experiments were conducted biannually at the start and end of the vegetation growing season in a surface flow wastewater treatment wetland located near Phoenix, AZ. Tracer experiments were conducted prior to and following reconfiguration and replanting of a 1.2 ha treatment wetland from its original design of alternating shallow and deep zones to incorporate hummocks (shallow planting beds situated perpendicular to flow). Tracer test data were analyzed using analysis of moments and the one-dimensional transport with inflow and storage numerical model to evaluate the effects of the seasonal vegetation growth cycle and hummocks on solute transport. Following reconfiguration, vegetation coverage was relatively small, and minor changes in spatial distribution influenced wetland hydraulics. During start-up conditions, the wetland underwent an acclimation period characterized by small vegetation coverage and large transport cross-sectional areas. At the start of the growing season, new growth of emergent vegetation enhanced hydraulic performance. At the end of the growing season, senescing vegetation created short-circuiting. Wetland hydrodynamics were associated with high volumetric efficiencies and velocity heterogeneities. The hummock design resulted in breakthrough curves characterized by multiple secondary tracer peaks indicative of varied flow paths created by bottom topography.

Citation: Keefe, S. H., J. S. (Thullen) Daniels, R. L. Runkel, R. D. Wass, E. A. Stiles, and L. B. Barber (2010), Influence of hummocks and emergent vegetation on hydraulic performance in a surface flow wastewater treatment wetland, *Water Resour. Res.*, *46*, W11518, doi:10.1029/2010WR009512.

1. Introduction

[2] Surface flow treatment wetlands are widely used to polish effluent from municipal, industrial, and agricultural wastewater treatment facilities by a complex interaction of physical, chemical, and biological processes that reduce concentrations of suspended solids, nutrients, dissolved organic carbon, volatile organic compounds, biochemical oxygen demand, and coliform bacteria [*Sartoris et al.*, 2000; *Barber et al.*, 2001; *Knowlton et al.*, 2002; *Kadlec*, 2003; *Keefe et al.*, 2004a; *Bastviken et al.*, 2009; *Kadlec*, 2009]. Hydraulic performance and system sustainability of treatment wetlands are a function of morphology and vegetative biomass, which facilitate transformation processes. Flow regimes with uniform velocity distributions provide ideal mixing and residence time, and hydraulic inefficiencies are caused by microtopography and spatially variable vegetation density which results in nonuniform flow resistance and incomplete mixing [*Kadlec and Knight*, 1996]. Wetland system design elements such as deep zones and islands situated perpendicular to the flow path can improve hydraulic performance by optimizing flow distribution and residence time [*Hammer and Knight*, 1994; *Persson*, 2000; *Knight et al.*, 2003; *Persson*, 2005; *Lightbody et al.*, 2007]. Other factors influencing treatment wetland hydrodynamics include system shape, aspect ratio, inlet and outlet structure design, water depth, and bottom roughness [*Thackston et al.*, 1987; *Somes et al.*, 1999; *Jenkins and Greenway*, 2005; *Wörman and Kronnäs*, 2005].

[3] Design features such as hummocks (shallow planting beds situated perpendicular to flow) can also be used to maintain vegetation balance by providing variable water depths for managing plant growth and decomposition [*Thullen et al.*, 2005]. Deep water surrounding the hummocks provides an opportunity for senesced vegetation to be inundated, allowing the decomposition process to release nutrients and create space for new growth [*Thullen et al.*, 2002]. Vegetation management using hummocks can promote higher dissolved oxygen in the water column, decreased internal nutrient loading, and better habitat for larvivorous fish and other mosquito predators [*Thullen et al.*, 2005].

[4] The hydraulic implications of hummocks have not been extensively studied. Hydraulic tracer tests have been used in wetlands to describe the residence time distribution (RTD) and hydraulic performance [*Stairs and Moore*, 1994; *Martinez and Wise*, 2003a; *Hodgson et al.*, 2004; *Dierberg and DeBusk*, 2005; *Persson*, 2005; *Wang et al.*, 2006; *Headley and Kadlec*, 2007]. Temporal moment and wetland efficiency analysis further describes the RTD and quantifies bulk wetland hydraulics [*Thackston et al.*, 1987; *Kadlec*, 1994; *Kadlec and Knight*, 1996; *Persson et al.*, 1999; *Jawitz*, 2004; *Kadlec*,

[1]U.S. Geological Survey, Boulder, Colorado, USA.
[2]U.S. Geological Survey, Denver, Colorado, USA.
[3]Wass Gerke and Associates, Inc., Scottsdale, Arizona, USA.
[4]Bureau of Reclamation, Denver, Colorado, USA.

Copyright 2010 by the American Geophysical Union.
0043-1397/10/2010WR009512

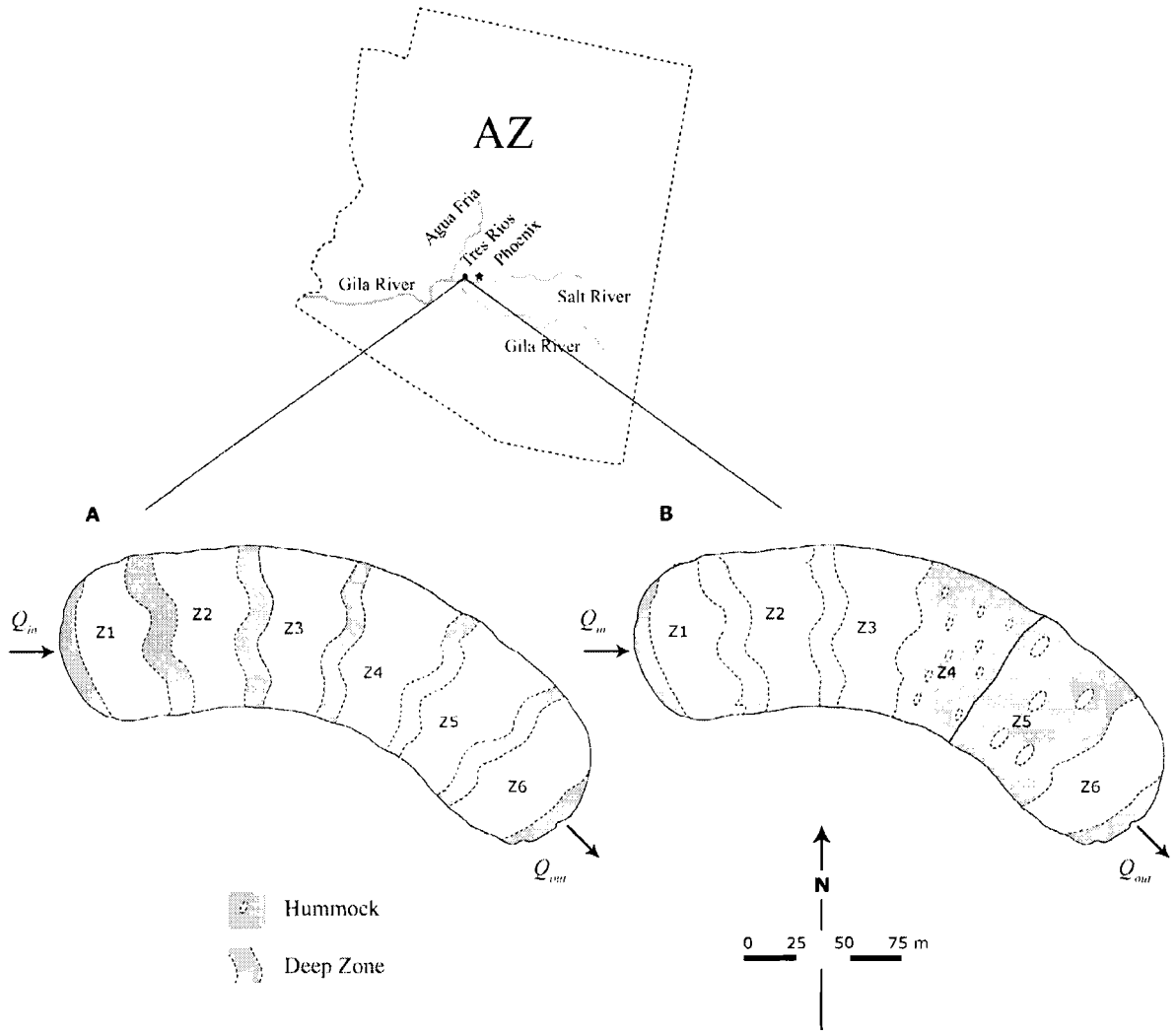

Figure 1. Schematic drawings of (a) preconfiguration conditions (winter 2002) and (b) postconfiguration conditions (fall 2003) at the Hayfield 1 wetland, located at the Tres Rios Wastewater Treatment Constructed Wetlands near Phoenix, AZ [Z1–Z6, zone 1 to zone 6; Q_{in}, inlet volumetric flow rate; Q_{out}, outlet volumetric flow rate].

2007, 2008]. The one-dimensional transport with inflow and storage (OTIS) numerical model [*Runkel*, 1998; http://co.water.usgs.gov/otis] has been applied to several wetland systems [*Martinez and Wise*, 2003b; *Keefe et al.*, 2004a, 2004b; *Harvey et al.*, 2005; *Wang and Jawitz*, 2006] and describes solute transport by advection and dispersion in active preferential flow pathways as well as exchange with transient storage areas in stagnant water and emergent vegetation zones. Numerically determined transport parameters and temporal moment analysis provide insight into treatment performance based on mixing characteristics.

[5] This manuscript describes an investigation of the relations between wetland system morphology, vegetation growth, and hydraulic efficiency at the Tres Rios Wastewater Treatment Constructed Wetlands located near Phoenix, AZ. A 1.2 ha wetland was reconfigured from six shallow emergent vegetation zones and five deep open-water zones to four bands of shallow emergent vegetation and two zones of hummocks surrounded by deep water. Tracer experiments and vegetation surveys were conducted over a 4 year period from the end of the growing season prior to reconfiguration, through three full growing seasons following reconfiguration. Analysis of the tracer tests conducted at the beginning (spring) and end (fall) of the growing seasons provided insight into transport characteristics of the wetland as a function of design elements and seasonal vegetation cycles.

2. Methods

2.1. Site Description

[6] The Tres Rios Constructed Treatment Wetlands are located at the 91st Avenue Wastewater Treatment Plant near the confluence of the Salt, Gila, and Agua Fria Rivers in Maricopa County, AZ (Figure 1). This facility serves the wastewater treatment needs of the greater Phoenix metropolitan area, with a treatment capacity of 1.4×10^8 L d^{-1}

Table 1. Tres Rios Hayfield 1 Wetland Configuration and Hydraulic Conditions During the Tracer Tests and Vegetation Surveys[a]

	W02	F03	S04	F04	S05	F05
Test Start Date	6 Dec 2002	30 Oct 2003	9 Apr 2004	26 Oct 2004	3 May 2005	25 Oct 2005
V_d (m^3)	6517	8510	8510	8510	8510	8510
A_d (m^2)	28.6	37.3	37.3	37.3	37.3	37.3
Q_{in} (m^3 s^{-1})	2.3×10^{-2}	2.3×10^{-2}	2.3×10^{-2}	2.4×10^{-2}	2.3×10^{-2}	2.3×10^{-2}
Q_{out} (m^3 s^{-1})	2.1×10^{-2}	1.9×10^{-2}	1.8×10^{-2}	2.0×10^{-2}	2.0×10^{-2}	2.0×10^{-2}
Q_{seep} (m^3 s^{-1})	1.3×10^{-3}	4.4×10^{-3}	3.1×10^{-3}	4.0×10^{-3}	1.7×10^{-3}	1.7×10^{-3}
Q_{evap} (m^3 s^{-1})	6.1×10^{-4}	2.7×10^{-4}	1.3×10^{-3}	6.3×10^{-4}	1.4×10^{-3}	8.0×10^{-4}
Fractional Recovery (%)	85	81	82	90	79	76

[a]W02, winter 2002; F03, fall 2003; S04, spring 2004; F04, fall 2004; S05, spring 2005; F05, fall 2005; V_d, design volume; A_d, average design cross-sectional area; Q_{in}, inlet volumetric flow; Q_{out}, outlet volumetric flow; Q_{seep}, groundwater seepage volumetric flow; Q_{evap}, evapotranspiration volumetric flow.

(179,000,000 gal. d^{-1}). The wetlands receive activated sludge treated wastewater that has undergone nitrification and denitrification followed by chlorination and dechlorination and has low biological oxygen demand, total suspended solids, and nutrient content [*Wass, Gerke and Associates*, 2001]. The north Hayfield 1 wetland was selected for this study because the emergent vegetation had degraded to a point it was not sustainable (dying off without regrowth). The wetland is approximately 1.2 ha (3 acres) in surface area, 228 m long, and 60 m wide [*CH2M Hill*, 1997]. Flow into the wetland and water depth is controlled by inlet and outlet structures fitted with v-notch weirs for discharge measurements. The kidney-shaped configuration was designed to simulate a riverine oxbow (Figure 1a).

[7] In the spring of 2003, the Hayfield 1 wetland was reconfigured. Four of the six shallow emergent vegetation zones (0.3 m deep during normal operations and 28 m in length) and all of the deep open water zones (1.3 m deep during normal operations and 9 m in length) were left as originally built. The surface of emergent vegetation zone 1 was scraped to remove existing plants, but zone 2, zone 3, and zone 6 were unaltered prior to replanting. Emergent zone 4 and zone 5 were reconfigured into hummocks of two different sizes (Figure 1b) by excavating soil around previously vegetated areas to a depth of about 1.5 m and leaving the hummock top in place. Zone 4 has 10 polygon-shaped hummocks (4.6 m × 2.3 m, 9.3 m^2 top area) with 3:1 slopes oriented perpendicular to flow. Zone 5 has five larger hummocks (9.1 m × 4.6 m, 37.3 m^2 top area). Soil was added to the top of some of the hummocks and compacted so that final elevations varied from 30 cm below to 10 cm above the normal operating surface. The shallow emergent vegetation areas of zone 1 and zone 6 were replanted with *Schoenoplectus tabernaemontani* (softstem bulrush) and *S. americanus* (Olney's bulrush) as was done originally in 1996. Emergent areas in zone 2 to zone 5 were planted with *S. acutus* (hardstem bulrush), *S. californicus* (giant bulrush), *S. tabernaemontani*, and *S. americanus*. *Typha domingensis* (southern cattail) was not planted but propagated on its own in many areas within the wetland. The net effect of reconfiguration was a ~20% increase in design volume and average cross-sectional area (Table 1; design volume estimated from drawings and drain and fill experiments) [*Wass, Gerke and Associates*, 2007].

2.2. Vegetation Sampling

[8] Aquatic plant culm (stem) density, diameters, and heights were measured by species and recorded from 22 representative 0.06 m^2 quadrants located throughout the treatment wetland prior to each tracer test to document plant growth and establishment. Representative vegetation biomass samples were taken each sampling period to quantify general biomass patterns by plant species. Live above-ground vegetation, dead above-ground vegetation (detritus), and live root/rhizome material within the quadrants were harvested, cleaned, and air dried until there was no further weight loss, and dry weight was converted to g m^{-2}. Vegetation coverage was quantified using georectified aerial photography (1:1500) and geographical information system (GIS) imagery to determine the surface area covered by each species during each tracer testing period. Percentage of areal vegetation coverage for each zone was verified by ground truthing. These verified coverage data were then multiplied by the mean culm density of each plant species for each sampling event to determine the total number of culms within each zone. These data were then used to compare vegetation growth between years and seasons.

2.3. Tracer Experiments

[9] During this investigation, a series of six tracer tests were conducted between 2002 and 2005. The first tracer test was conducted during the winter of 2002 (W02) under the original configuration (Figure 1a). Following reconfiguration (Figure 1b) in the spring of 2003, tracer tests were conducted at the end of the first growing season (fall 2003, F03), the start (spring 2004, S04) and end (fall 2004, F04) of the second growing season, and the start (spring 2005, S05) and end (fall 2005, F05) of the third growing season. Approximately 100 kg of sodium bromide (Alameda Chemical, Oakland, CA) was mixed in a 250 L polyethylene barrel containing influent water until completely dissolved and then pumped into the inlet splitter box. The tracer cloud was discharged into the wetland through a subsurface manifold pipe that spreads flow laterally across the inlet deep zone, transverse to the direction of flow.

[10] Volumetric flow (Q) at the wetland inlet (Q_{in}) and outlet (Q_{out}) were determined from measured water levels over v-notch weirs (Sutron Accubar 5600 with Xlite 9210 data logger, Sterling, VA) and flow rating curves. Steady state flow conditions were maintained for the duration of each tracer experiment at a constant hydraulic loading rate (HLR = 15 cm d^{-1}) and a 0.3 m emergent vegetation zone depth. Flow decreases ($Q_{out} < Q_{in}$) were attributed to evapotranspiration (Q_{evap}) and groundwater seepage (Q_{seep}) (Table 1). Evapotranspiration loss was estimated using data from the Litchfield and Buckeye weather stations (http://ag.arizona.

edu/azmet) and groundwater seepage was estimated by difference ($Q_{out} = Q_{in} - Q_{evap} - Q_{seep}$; Table 1).

[11] Prior to the start of the tracer tests, baseline water samples were collected in 125 mL plastic bottles at inlet and outlet locations. During each tracer test, water samples were collected at the wetland outlet every hour (by autosampler, American Sigma, model 1350, Loveland, CO) for the first 2 weeks and every 4–6 h during the second and third week of the experiment. Dissolved bromide concentrations were determined by ion chromatography [*Pfaff et al.*, 1997]. During the course of the six experiments, the quality assurance program consisted of laboratory blanks and duplicate analyses of field samples. Bromide analysis had a detection limit of 0.3 mg L^{-1}, the laboratory blanks (n = 350) were below the reported detection limit, and the average relative percent difference for duplicate samples (n = 423) was 2%.

[12] Fractional recovery of the bromide tracer was determined by integrating the concentration-flow time series at the wetland outlet after correcting for the background bromide concentration ($C_{background}$) and tracer loss due to groundwater seepage,

$$\text{fractional recovery} = \frac{\int_0^t (C_{out} - C_{background}) Q_{out} \mathrm{d}t}{m - \int_0^t C_{seep} Q_{seep} \mathrm{d}t}, \quad (1)$$

where m is mass of tracer added (mg), t is time (s), and C_{seep} is the tracer concentration associated with groundwater seepage (mg L^{-1}), as given by the average of the inlet (C_{in}) and outlet (C_{out}) concentrations,

$$C_{seep} = 0.5(C_{in} + (C_{out} - C_{background})), \quad (2)$$

$$C_{in} = \frac{m}{\int_0^t Q_{in} \mathrm{d}t}. \quad (3)$$

Fractional recoveries less than 1.0 (Table 1) indicate a loss of bromide that is attributable to experimental uncertainties in wetland tracer tests [*Chendorain et al.*, 1998; *Lin et al.*, 2003]. Outlet tracer concentration data were therefore scaled to account for bromide loss [*Atkinson and Davis*, 2000],

$$C_{scaled} = C_{out}/\text{fractional recovery}, \quad (4)$$

where C_{scaled} is the scaled tracer concentration (mg L^{-1}) used in the subsequent moments analysis and solute transport modeling.

2.4. Wetland Hydrodynamics

[13] Enhanced hydraulic performance of constructed wetlands is attributed to full utilization of the design volume, uniform velocity distributions, and approximate plug flow conditions [*Persson et al.*, 1999] (plug flow refers to an idealized situation in which tracer mass travels through the wetland with negligible mixing and dispersion). These desirable attributes are assessed herein using both conventional approaches based on the method of moments [e.g., *Kadlec*, 1994, section 2.4.1] and solute transport modeling [e.g., *Keefe et al.*, 2004b, section 2.4.2]. Hydraulic performance is evaluated relative to seasonal changes in emergent vegetation coverage during wetland maturation from start-up conditions and before and after modification of the wetland morphology with hummocks (section 3).

2.4.1. Method of Moments

[14] In order to compare tracer experiments conducted in varied volumes and flow regimes, a dimensionless "flow-weighted time RTD function" [*Werner and Kadlec*, 1996; *Headley and Kadlec*, 2007] was used to express a normalized concentration ($C'(\phi)$) as a function of a dimensionless flow weighted time (ϕ),

$$C'(\phi) = \frac{C_{out}(t) V_d}{M_{out}}, \quad (5)$$

$$\phi = \frac{V_{out}}{V_d}, \quad (6)$$

where M_{out} (g) and V_{out} (m^3) are the total mass and the cumulative volume that has exited the wetland since the tracer addition, respectively, and V_d is the design volume (m^3).

[15] The distribution of tracer concentrations may be described by a series of temporal moments [*Kadlec*, 1994]. Using the method of moments, the mean hydraulic residence time (τ) is defined as the centroid of the observed tracer breakthrough curve (the first moment about zero). The variance (σ^2) characterizes the spread of the breakthrough curve about the mean of the distribution (the second central moment) and is a measure of the degree of mixing or distribution of velocities. A dimensionless variance (σ_θ^2) is given by *Kadlec* [1994] and *Nauman* [2008],

$$\sigma_\theta^2 = \frac{\sigma^2}{\tau^2}. \quad (7)$$

The τ determined from the moment analysis of observed tracer data may be compared to the theoretical hydraulic residence time that would be observed in the absence of mixing (plug flow). Nominal hydraulic residence time (τ_n) under ideal plug flow conditions is calculated as the simple ratio of wetland volume and flow,

$$\tau_n = \frac{V_d}{Q_{avg}}, \quad (8)$$

where Q_{avg} is the average flow rate (= $(Q_{in} + Q_{out})/2$).

2.4.2. Solute Transport Modeling

[16] Physical transport processes in streams are often quantified by calibrating a one-dimensional solute transport model to tracer breakthrough curves [e.g., see *Runkel et al.*, 2003, and references therein]. One-dimensional models of solute transport typically consist of an advective term to describe bulk transport in the downstream direction and a dispersion term to describe mixing due to variations in the velocity field. Dispersive mixing may not adequately describe the observed spreading of solutes in many streams, as some of the tracer is detained in slow moving areas adjacent to the main channel. The failure of the one-dimensional advection-dispersion equation to describe solute mixing has been widely noted in the literature for stream systems, and alternate models that include the process of transient storage have been developed [*Bencala and Walters*, 1983]. Use of the transient storage model represents a compromise between a strictly one-dimensional approach and a two-dimensional model and is quasi-two dimensional, with the transient storage zone representing the second dimension.

[17] The elongated shape of the Hayfield 1 wetland (aspect ratio = length/width = 3.8) and its well-defined inlet and outlet structures result in a flow field that is predominately one dimensional. As such, the one-dimensional modeling approach described above for streams may be reasonable for quantifying wetland hydraulics. To this end, the transient storage model OTIS [*Runkel*, 1998] is used herein to assess hydraulic performance. Within OTIS, the wetland is conceptually divided into two areas: the main channel and the storage zone. The main channel represents areas of the wetland in which advection is the dominant transport mechanism, and the storage zone represents stagnant water areas (e.g., quiescent pools surrounded by emergent vegetation). Governing equations for the main channel and transient storage zone are [*Runkel*, 1998; *Keefe et al.*, 2004b]

$$\frac{\partial C}{\partial t} = -\frac{Q}{A}\frac{\partial C}{\partial x} + \frac{1}{A}\frac{\partial}{\partial x}\left(AD\frac{\partial C}{\partial x}\right) + \frac{Q_{\mathrm{evap}}}{A}(C) + \alpha(C_{\mathrm{S}} - C), \quad (9)$$

$$\frac{\mathrm{d}C_{\mathrm{S}}}{\mathrm{d}t} = \alpha\frac{A}{A_{\mathrm{s}}}(C - C_{\mathrm{S}}), \quad (10)$$

where C and C_{S} are tracer concentrations in the main channel and storage zones (mg L^{-1}), x is distance downstream from the input (m), Q_{evap} is the rate of evapotranspiration per unit length L (= Q_{evap}/L; $\mathrm{m}^3\ \mathrm{s}^{-1}\ \mathrm{m}^{-1}$), A is main channel cross-sectional area (m^2), D is longitudinal dispersion ($\mathrm{m}^2\ \mathrm{s}^{-1}$), α is storage zone exchange rate (s^{-1}), and A_{s} is storage zone cross-sectional area (m^2).

[18] Application of equations (9) and (10) requires specification of an upstream boundary condition in terms of the tracer concentration at the wetland inlet. The upstream boundary concentration was set equal to wetland inlet concentration for all times before and after the tracer addition. During tracer addition, the boundary concentration was set equal to the concentration that would result from mixing of the wastewater effluent with the injected tracer at the wetland inlet.

[19] OTIS was calibrated to the wetland outlet breakthrough curves to estimate transport parameters that characterize wetland hydraulics. This single-reach approach is identical to many stream applications in which the model is calibrated to tracer data collected at the reach endpoint. In a typical stream application, reach lengths are on the order of 100–500 m, with each reach being subdivided into a number of segments (control volumes; ~1–3 m in length) for which the governing equations are solved. Because of within-reach heterogeneity, physical characteristics such as cross-sectional area vary with length. Measurement of average cross-sectional area, for example, would require numerous transects to obtain representative values for the entire reach. Alternatively, model calibration provides a means to develop parameter estimates that represent average conditions within the reach (e.g., cross-sectional areas estimated via calibration represent average values integrated over the length of the wetland).

[20] Model calibration entails the development of hydraulic parameter estimates (A, A_{s}, α, and D) that produce a close correspondence between simulated and observed concentrations. This parameter estimation process was facilitated by OTIS-P, a version of OTIS that uses nonlinear regression to minimize the squared differences between simulated and observed concentrations (residual sum of squares) [*Runkel*, 1998]. Application of OTIS-P to each tracer data set was initially based on a simple advection-dispersion model in which transient storage was not considered (A and D were estimated). This initial application was followed by an additional OTIS-P simulation in which the processes of advection, dispersion, and storage were considered (A, A_{s}, α, and D were estimated). The more complex model was used to qualitatively investigate the hydraulic effects of the addition of transient storage (see section 3.6).

2.4.3. Hydraulic Performance

[21] Parameters estimated using the method of moments and solute transport modeling may be used to quantify hydraulic performance. Hydraulic performance is evaluated in terms of (1) utilization of the design volume and (2) velocity uniformity and plug flow.

2.4.3.1. Utilization of Design Volume

[22] In wetland systems, ideal plug flow conditions rarely exist. Water parcels traveling through a wetland follow a hydraulic RTD described by the tracer breakthrough curve [*Danckwerts*, 1953; *Levenspiel*, 1972; *Fogler*, 1992; *Kadlec and Knight*, 1996; *Headley and Kadlec*, 2007]. This departure from plug flow conditions results in a discrepancy between the theoretical τ_{n} (equation (8)) and the observed τ parameters, which can be used to define volumetric efficiency (e_{V}), the wetland volume that is effective in the treatment process [*Thackston et al.*, 1987; *Persson*, 2005; *Kadlec*, 2007, 2008],

$$e_{\mathrm{V}} = \frac{\tau}{\tau_{\mathrm{n}}}. \quad (11)$$

An alternative means of quantifying volume utilization is to compare cross-sectional areas developed via transport modeling (A) with the design cross-sectional area (A_{d}). The ratio of modeled and design areas provide a numerical value that is analogous to the volumetric efficiency,

$$e_{\mathrm{V\text{-}mod}} = \frac{A}{A_{\mathrm{d}}}, \quad (12)$$

where $e_{\mathrm{V\text{-}mod}}$ is the modeled volumetric efficiency.

2.4.3.2. Velocity Uniformity and Plug Flow

[23] Enhanced hydraulic performance is thought to occur when plug flow conditions are approximated. Plug flow conditions arise when the velocity distribution is uniform, resulting in negligible mixing and dispersion. Hydraulic performance is thus maximized when transport through the wetland approaches that of an idealized Plug Flow Reactor (PFR) [*Chapra*, 1997]. Minimum hydraulic performance, in contrast, occurs when the wetland acts as a single, completely mixed system (i.e., Continuously Stirred Tank Reactor, CSTR). Wetland transport may be characterized using moment analysis and the parameter N, the number of CSTRs within the system [*Fogler*, 1992; *Kadlec*, 1994],

$$N = \frac{\tau^2}{\sigma^2}. \quad (13)$$

The number of CSTRs may in turn be used to determine the efficiency of the detention time distribution, DTD (e_{DTD}) [*Kadlec*, 1994, 2007, 2008],

$$e_{\mathrm{DTD}} = \left(1 - \frac{1}{N}\right). \quad (14)$$

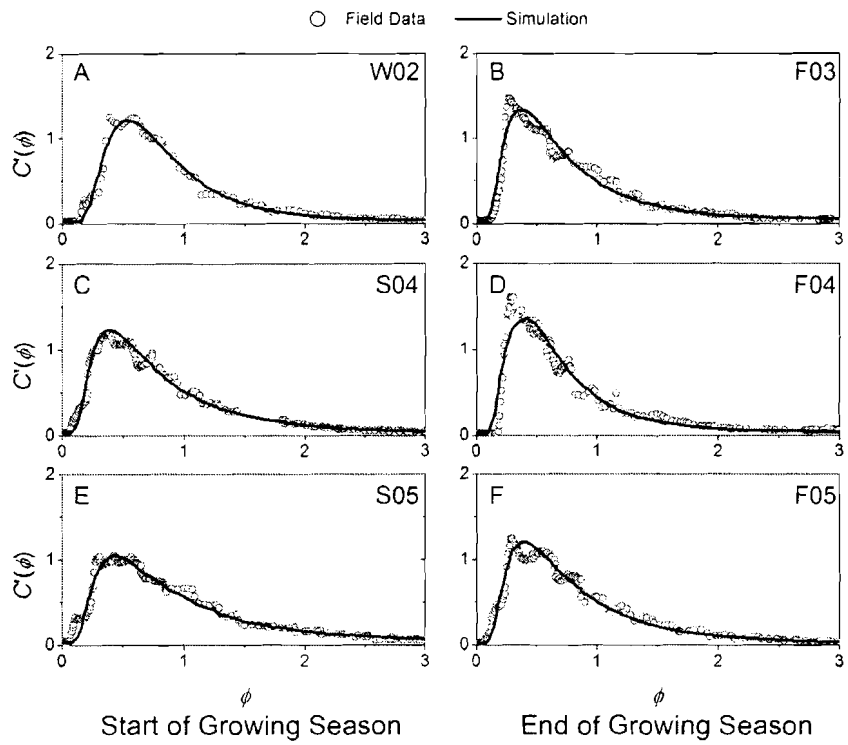

Figure 2. Normalized concentration ($C'(\phi)$) as a function of dimensionless flow weighted time (ϕ) for bromide tracer test data and OTIS simulations of observed breakthrough curves. Tracer experiments were conducted at the Hayfield 1 constructed wetland before and after reconfiguration to include the hummock design [W02, winter 2002 (original banded configuration); F03, fall 2003 (first year); S04, spring 2004; F04, fall 2004 (second year); S05, spring 2005; F05, fall 2005 (third year)].

As given by equations (13) and (14), plug flow conditions and enhanced hydraulic performance will be realized when N is large and e_{DTD} is close to unity (as N becomes large, wetland transport approaches that of a PFR and e_{DTD} approaches 1.0). The distinction between a plug flow system and completely mixed conditions also may be made based on the Peclet number (Pe), the dimensionless ratio of advective and dispersive transport [*Kadlec and Knight*, 1996]:

$$\sigma_\theta^2 = \left(\frac{2}{Pe}\right) - 2\left(\frac{1}{Pe}\right)^2 \left[1 - e^{-Pe}\right], \qquad (15)$$

where a large value of Pe (>10) indicates the system approaches a PFR and a low value (<0.1) indicates the system approaches a single CSTR.

3. Results and Discussion

3.1. Solute Transport Modeling

[24] Model simulations of the tracer breakthrough curves reproduce features of the observed data (Figure 2). In general, there is a close correspondence between the model results and the tracer peak, as well as initial breakthrough and tail, and the simple advection-dispersion model provides an adequate fit for all tracer experiments. During the first two fall periods following reconfiguration (F03, F04), the simple advection-dispersion model fails to reproduce the fronting behavior of the breakthrough curve (Figures 2b and 2d).

[25] Model parameters estimated by nonlinear regression and the associated coefficients of variation (COV) are shown in Table 3. The COV is defined as the standard deviation of the parameter estimate divided by the estimate and is a measure of parameter uncertainty [*Wagner and Harvey*, 1997; *Harvey et al.*, 2005]. Values of COV for A for all time periods are approximately 1%–2%, indicating a low level of uncertainty. This low level of uncertainty is due to the presence of A in the advection term of equation (9); A controls the velocity of the tracer cloud and is well defined by the tracer breakthrough [*Harvey and Wagner*, 2000]. The D estimates also have low COV values, ranging from 2% to 3% (Table 3). Parameter uncertainty in all cases is relatively low, lending credence to the modeling approach (COV < 3% is low relative to other studies; e.g., the parameter estimates reported by *Runkel* [1998] have COV values ranging from 9% to 37%).

[26] Further confidence in the model calibration may be obtained by comparing the parameter estimates with physically measurable quantities. The modeled volumetric efficiency ($e_{V\text{-}mod}$, equation (12), Table 3) ranged from 72%–94%, indicating that the modeled A is approximately equal to A_d. Values of $e_{V\text{-}mod}$ < 100% reflect the decrease in A_d that is attributable to vegetation growth. Another physical check on the modeled areas is provided by a comparison of simulations before and after reconfiguration. As shown in

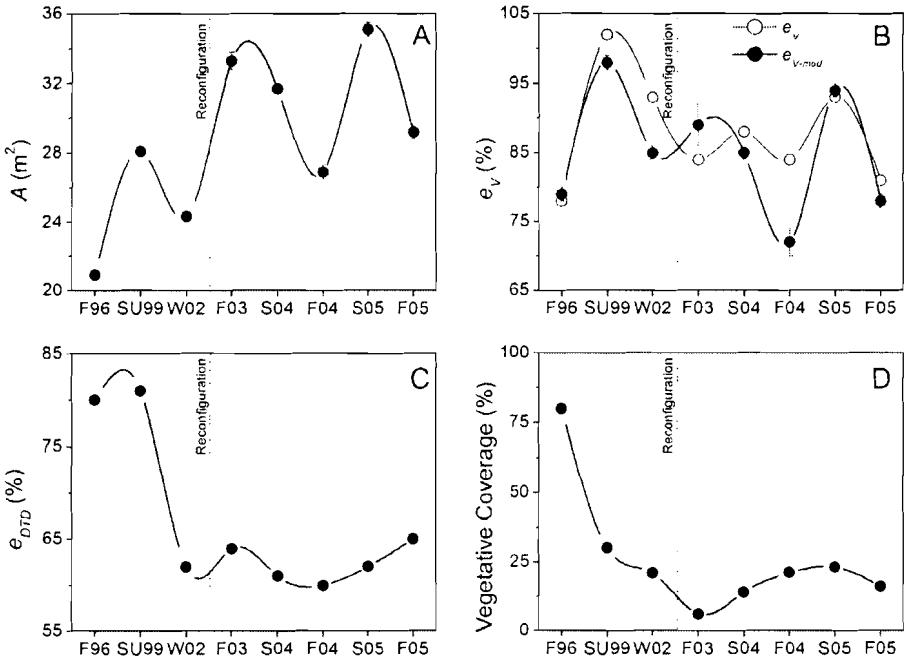

Figure 3. Changes in hydraulic parameters at the Hayfield 1 constructed wetland as a function of time: (a) numerically determined main channel cross-sectional area (A), (b) volumetric efficiency ($e_V = \tau/\tau_n$) and modeled volumetric efficiency ($e_{V\text{-mod}} = (A/A_d)$, (c) detention time distribution (DTD) efficiency (e_{DTD}), and (d) emergent vegetation coverage as a function of total wetland surface area [A_d, design cross-sectional area; τ, hydraulic residence time; τ_n, nominal hydraulic residence time; F96, fall 1996; SU99, summer 1999; W02, winter 2002; F03, fall 2003; S04, spring 2004; F04, fall 2004; S05, spring 2005; F05, fall 2005].

Figure 3a, the modeled A increases after reconfiguration, consistent with the increase in V_d and A_d (Table 1).

3.2. Morphology Effects

[27] The wetland was reconfigured from the original shallow emergent vegetation configuration to include two zones of hummocks (Figure 1). The positively skewed, pre-reconfiguration breakthrough curve with an extended tail is typical for a system dominated by advective transport as in the original shallow emergent vegetation configuration (Figure 2a). Changes in the shape of the breakthrough curves following reconfiguration (Figures 2b–2f), including temporally reproducible secondary peaks on the falling limb, are characteristics of tortuous flow paths not present before the reconfiguration. The shape of the breakthrough curves indicated varied velocity profiles and nonideal flow patterns (deviation from plug flow).

[28] Figure 3 depicts the hydraulic parameters A, e_V, $e_{V\text{-mod}}$, and e_{DTD} and vegetation coverage for the study tracer tests (W02, F03, S04, F04, S05, F05) as well as previously published tracer experiments (fall 1996, F96; summer 1999, SU99) [*Keefe et al.*, 2004b; *Kadlec*, 2008]. Reconfiguration to include hummocks increased the effective volume by 20%, which also is reflected in the hydraulic residence times (Table 2) that increased 21% ± 2% accordingly. Additionally, the flow-weighted time RTD function ($C'(\phi)$) shows general agreement before and after the reconfiguration (Figure 2). In the hummock design, the average e_V values (86% ± 5%) are comparable to ponds with good hydraulic efficiency resulting from distributed inflow (e_V = 0.89) [*Persson et al.*, 1999]. The reconfiguration did not significantly influence the e_V, $e_{V\text{-mod}}$, or e_{DTD} parameters (Figures 3b and 3c).

3.3. Emergent Vegetation Coverage and Biomass

[29] Emergent vegetation coverage changes through time are presented as a function of the entire wetland area in Figure 3d and by zone in Figure 4. Figure 3d shows a vege-

Table 2. Temporal Moment Analysis and Hydraulic Efficiency Parameters Determined From Tracer Tests Conducted at the Tres Rios Hayfield 1 Wetland[a]

	W02	F03	S04	F04	S05	F05
Moment and Residence Times						
τ (day)	3.27	3.95	4.24	3.77	4.19	3.69
σ_θ^2	0.375	0.362	0.394	0.402	0.376	0.351
τ_n (day)	3.50	4.68	4.81	4.49	4.50	4.56
Derived Values						
e_V (%)	93	84	88	84	93	81
e_{DTD} (%)	63	64	62	60	63	66
N	2.7	2.8	2.5	2.5	2.7	2.9
Pe	4.03	4.24	3.75	3.64	4.02	4.42

[a]W02, winter 2002; F03, fall 2003; S04, spring 2004; F04, fall 2004; S05, spring 2005; F05, fall 2005; τ, hydraulic residence time; σ_θ^2, dimensionless variance; τ_n, nominal hydraulic residence time; e_V, volumetric efficiency; e_{DTD}, detention time distribution efficiency; N, number of continuous stirred tank reactors; Pe, Peclet number.

Table 3. Solute Transport Parameters and Derived Quantities Determined Using the One-Dimensional Transport With Inflow and Storage (OTIS) Model to Analyze Tracer Tests Conducted at the Tres Rios Hayfield 1 Wetland[a]

	W02	F03	S04	F04	S05	F05
Model Parameters						
A (m^2)	24.3 (1)	33.3 (1)	31.7 (1)	26.9 (2)	35.1 (1)	29.2 (1)
D (m^2 s^{-1})	3.0×10^{-2} (2)	3.8×10^{-2} (2)	3.7×10^{-2} (2)	3.5×10^{-2} (3)	3.7×10^{-2} (2)	3.8×10^{-2} (2)
Derived Values						
u (m s^{-1})	8.9×10^{-4}	6.3×10^{-4}	6.5×10^{-4}	8.1×10^{-4}	6.2×10^{-4}	7.4×10^{-4}
$e_{V\text{-mod}}$ (%)	85	89	85	72	94	78

[a]W02, winter 2002; F03, fall 2003; S04, spring 2004; F04, fall 2004; S05, spring 2005; F05, fall 2005; A, main channel cross-sectional area; D, longitudinal dispersion coefficient; values in parentheses following A and D are percent coefficient of variation (COV) from nonlinear regression; u, velocity (equal to Q_{avg}/A, where $Q_{avg} = (Q_{in} + Q_{out})/2$); $e_{V\text{-mod}}$, modeled volumetric efficiency.

tation die-off between 1996 (F96) and 2002 (W02) in the original banded vegetation configuration. *Kadlec* [2008] noted stable emergent vegetation in the Hayfield 1 wetland until a vegetation die-off in the spring of 1998.

[30] During the study period, vegetation growth was slow compared to other southwestern treatment wetlands [*Sartoris et al.*, 2000] but generally followed an abridged sigmoidal curve through the beginning of the third growing season when coverage began to decline (Figures 3d and 4). Rapid vegetation growth in treatment wetlands usually occurs during the spring as new shoots emerge with increasing temperatures and as nutrients are absorbed from decomposed detritus. Vegetation coverage is maximized by the end of the growing season, followed by senescence of plants each fall as temperatures, day length, and nutrient uptake decrease [*Cronk and Fennessy*, 2001]. At maximum coverage (S05), the majority of the emergent vegetation grew in zone 1 and zone 6 (Figure 4). Zone 2 and zone 3 had considerably less vegetation coverage at peak growth. The hummocks reduced the available area for emergent growth in zone 4 by 96% and in zone 5 by 91% (total wetland by 34%). The emergent vegetation in zone 4 and zone 5 reached its peak growth at the end of the first growing period (F04).

[31] Biomass was not collected and measured from every vegetation sample but was taken as representative data to quantify the nondestructive sampling parameters [*Daniels et al.*, 2010] as needed. On the basis of those representative samples, the percentage of dead above-ground vegetation relative to live above-ground vegetation provided general comparisons for estimating percent detritus during each of the sampling periods. During W02 the percentage of dead to live culms was 31%; following reconfiguration and planting in F03 there were 0% dead to live culms; and subsequently, 1.5%, 9.5%, 6.4%, and 24% detritus was measured during S04, F04, S05, and F05, respectively.

[32] *Nepf* [1999] noted that mechanical diffusion (lateral displacement of flow due to emergent vegetation) dominates overall diffusion for systems where the solid plant fraction (SPF) or the projected plant area per unit volume (culm density × culm diameter^2) is greater than $O(0.1)$ (O, order of) or when the stem Reynolds number ($Re_d = u \times$ culm diameter$/\nu$, where u is the velocity and ν is the kinematic viscosity) $< \approx 200$. During the study period, the Re_d values averaged 2–21, comparable to other field values reported at Tres Rios of 5–20 [*Serra et al.*, 2004]. During W02, the SPF was 0.3 ± 0.2; following reconfiguration and planting in F03 the SPF declined an order of magnitude (0.03 ± 0.02). In the subsequent two growing periods (S04 through F05), the SPF values were not statistically different and averaged 0.3 ± 0.2.

[33] After the vegetation die-off, the hydraulic parameters indicated a decrease in wetland performance for both wetland configurations (Table 2). The wetland was functioning as a PFR ($Pe = 8.8 \pm 0.3$, $N = 5.0 \pm 0.2$) until 1999 (F96, SU99). By the start of this study period (W02), the mean Pe (4.0 ± 0.3) and mean N (2.7 ± 0.2) values indicated a transitional flow between a PFR and a CSTR [*Chapra*, 1997]. After vegetation die-off, the e_{DTD} values decreased significantly with the exception of SU99 (Figure 3c), where elevated e_V values indicated that overall vegetation coverage did not control mixing and preferential flow paths. *Kadlec* [2008] showed a similar decrease in N, e_V, and e_{DTD} between 1998 and 2001 after the vegetation die-off in the Hayfield 1 wetland.

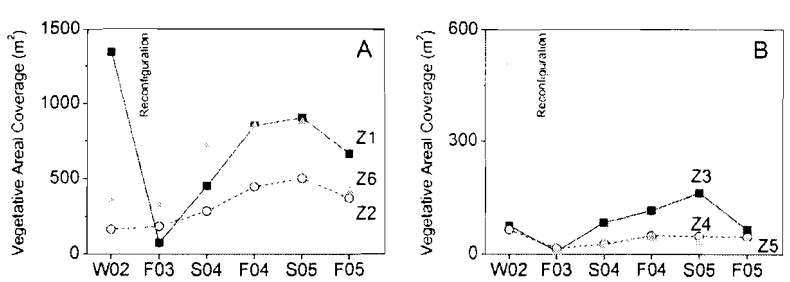

Figure 4. Areal vegetation coverage as a function of (a) zone 1, zone 2, and zone 6 and (b) zone 3, zone 4, and zone 5 at the Hayfield 1 constructed wetland [Z1–Z6, zone 1–zone 6; W02, winter 2002; F03, fall 2003; S04, spring 2004; F04, fall 2004; S05, spring 2005; F05, fall 2005].

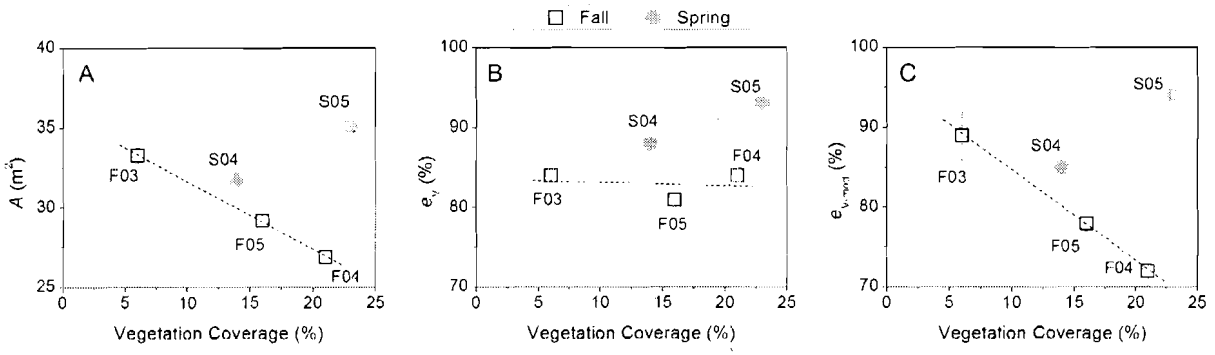

Figure 5. Changes in hydraulic parameters at the Hayfield 1 constructed wetland as a function of vegetation coverage in the postreconfiguration hummock conditions: (a) numerically determined main channel cross-sectional area (A), (b) volumetric efficiency ($e_V = \tau/\tau_n$), and (c) modeled volumetric efficiency ($e_{V\text{-mod}} = (A/A_d)$) [$A_d$, design cross-sectional area; τ, hydraulic residence time; τ_n, nominal hydraulic residence time].

3.4. Seasonal Effects

[34] During the study period, there was a seasonal relation in the breakthrough curves (Figure 2) between the start (S04 and S05) and end (F03, F04, and F05) of the growing season. A sharp fronting behavior occurred at the end of the first two growing seasons (Figures 2b and 2d), where short-circuiting appears to dominate solute transport. A rapid peak and long tail for the breakthrough curves indicates short-circuiting, dead zones with small advective flow areas, and relatively little longitudinal dispersion [*Thackston et al.*, 1987; *Martinez and Wise*, 2003b]. Velocity heterogeneities have been widely reported in constructed wetlands [*Persson et al.*, 1999; *Wörman and Kronnäs*, 2005; *Lightbody et al.*, 2008].

[35] Following wetland reconfiguration, there was an acclimation period (F03) characterized by larger values for A (Figure 3a) and significant fronting of the tracer response curve (Figure 2b). During the first growing season (F03), short-circuiting occurred due to the sparse vegetation (SPF ≈ 0.001–0.10) as the newly planted shoots were beginning to establish (Figure 4). The hydrodynamic effects of relatively sparse emergent vegetation (SPF ≈ 0.001–0.10) and low stem Reynolds number ($Re_d \approx 5$–20) have not been extensively studied. Conditions at the end of the second and third growing seasons (F04 and F05) were characterized by accumulation of detritus and lodging of senescent vegetation. Generally, the fall transport simulations had lower A, e_V, and $e_{V\text{-mod}}$ values (Figure 3). *Persson* [2005] showed a similar seasonal trend for e_V, with lower values in the winter and higher values in the summer. In the fall, A and $e_{V\text{-mod}}$ values decreased with increasing vegetation cover (Figure 5).

[36] At the end of the third growing season (F05), the fronting behavior of the tracer response curve was less pronounced and the total number of live culms declined (39%) compared to the start of the growing season. A large amount of the resulting detritus (24%) remained upright without lodging, decreasing the hydraulic resistance effect. Decreases in velocity, discharge, and boundary shear stress due to emergent vegetation have been noted [*Oldham and Sturman*, 2001; *Stern et al.*, 2001; *Sun and Shiono*, 2009].

[37] Typically in the spring, new shoots emerge from root stock and are more likely to interact with flow paths and enhance hydraulic performance. The spring breakthrough curves (Figures 2c and 2e) generally have longer τ values compared to the end of the growing season (Table 2). The decay limb of the spring breakthrough curves declined at a slower rate and returned to background concentrations at a later time than the fall curves. Although only two sampling events were conducted in the spring, general trends indicate A, e_V, and $e_{V\text{-mod}}$ increased with time (Figures 3a and 3b) and vegetation cover (Figure 5).

3.5. Vegetation Spatial Distribution

[38] Because hydraulic heterogeneities cannot be fully explained by changes in overall vegetation coverage, it is important to explore the effect of vegetation spatial distribution within the wetland. The vegetation influence on hydraulics resulted mainly from changes in zone 1 and zone 6 during the second and third growing seasons.

[39] In the second growing season (S04, F04), the hydraulics were influenced mostly by an increase of vegetation coverage in zone 1. In the spring, vegetation coverage had increased from F03 but was still sparse (SPF ~ 0.2–0.3; Figure 6a). Using a three-dimensional sampling network, *Williams and Adamsen* [2008] showed a predominant short-circuit pathway in zone 1 and uniform mixing both laterally and vertically near the outlet during the S04 experiment. By the F04 survey (Figure 6b), the vegetation nearly doubled in zone 1 (from 451 to 854 m^2). Additionally, lodged detritus had built up to 9.5% throughout the entire wetland creating higher flow resistance characterized by fronting of the tracer cloud and hydraulic focusing (Figure 2d). *Burke and Wadzuk* [2009] noted that nonuniform longitudinal velocities resulted from variations in bottom topography and detritus.

[40] Vegetation coverage at the start of the third growing season (S05, 23%) was comparable to the end of second growing season (F04, 21%; Figure 3d) but exhibited different hydraulic characteristics (Figures 2d and 2e) likely due to three vegetation patterns: (1) a thick cover of *Lemna* spp. (duckweed) occurred in F04 but not in S05, (2) much of the lodged F04 detritus had decomposed by spring, and (3) little new growth emerged in S05. The seasonal influence on hydraulics during the third growing season began similarly to S04 (Figures 2c and 2e); however as overall

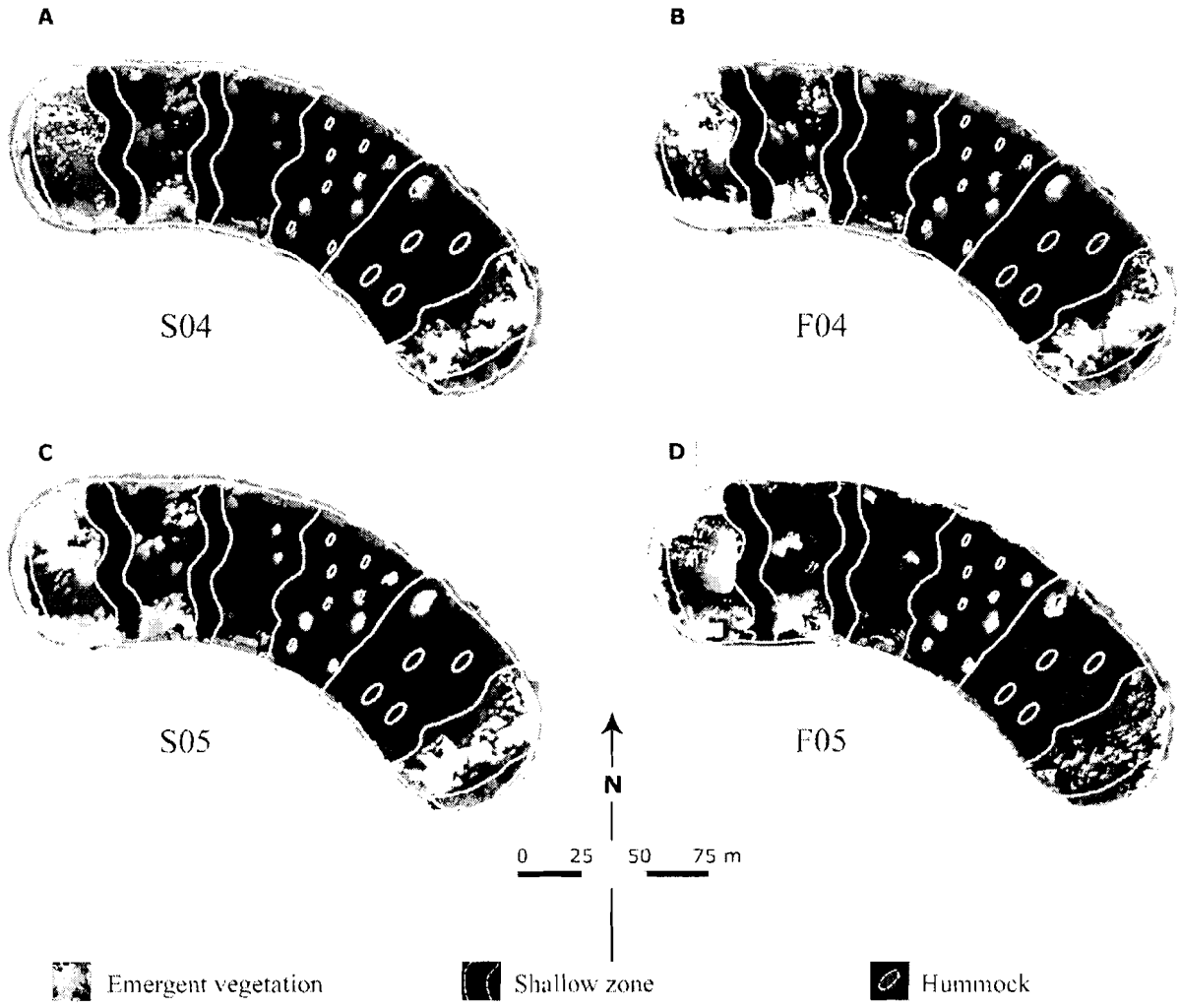

Figure 6. Aerial photography-based vegetation coverage of the Hayfield 1 wetland during tracer experiments conducted in (a) the spring of 2004, S04; (b) the fall of 2004, F04; (c) the spring of 2005, S05; and (d) the fall of 2005, F05.

vegetation decreased through the growing season, hydraulic control was influenced by zone 6 with secondary influences by zone 1 (27% loss occurring in zone 1 and 51% loss in zone 6 relative to the spring vegetation coverage; Figures 4 and 6). During the S05 survey, the band of live upright emergent vegetation from the previous season's growth across zone 6 (Figure 6c) created hydraulic resistance that likely reduced the flow velocity and enhanced mixing. By the F05 survey, zone 6 contained more open areas due to the limited new growth and extensive die-off (Figure 6d), covering only 51% of the area it had in F04. Additionally, aerial photography of zone 1 shows two unvegetated areas that likely acted as transport corridors and reduced short-circuiting in the early stages of the wetland (F05).

3.6. Benefits and Limitations of Modeling Approach

[41] As shown in this study and elsewhere [*Martinez and Wise*, 2003b; *Keefe et al.*, 2004a, 2004b], one-dimensional models such as OTIS provide a means to quantify hydraulic performance in constructed wetlands. Objective measures for quantifying the utilization of design volume and the uniformity of the velocity field have been presented herein as an alternative to measures based on the method of moments. For the case of volume utilization, $e_{V\text{-mod}}$ is proposed, and values of $e_{V\text{-mod}}$ compare favorably with moment-based e_V values (Figure 3b). The utility of the modeling approach to quantify nonuniformities in the velocity field is less clear-cut, given the low levels of transient storage in transport simulations. Transient storage in constructed wetlands has been used to distinguish between areas of active flow (the main channel) and low-velocity water (the storage zone) [*Martinez and Wise*, 2003b; *Keefe et al.*, 2004a, 2004b]. Although not discussed herein, the ability to distinguish between the main channel and the storage zone may have important ramifications for the study of reactive substances as these two areas can have significantly different biogeochemical characteristics [*Runkel et al.*, 2003; *Keefe*

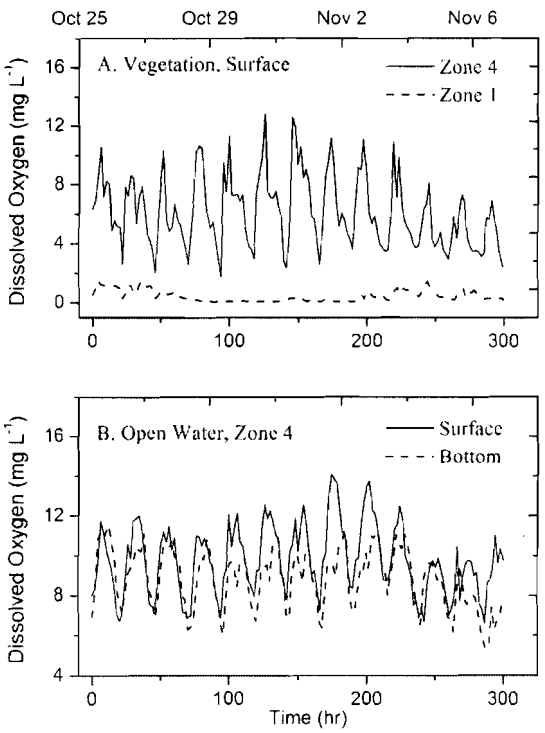

Figure 7. Dissolved oxygen concentrations during the fall 2005 tracer test at the Hayfield 1 constructed wetland in (a) the emergent vegetation on a hummock (zone 4) and in the shallow emergent vegetation (zone 1) and (b) the open water (zone 4) near the surface and bottom.

et al., 2004a]. Similar zones of diverse water quality exist within the Hayfield 1 wetland.

[42] During the F05 tracer test, in situ dissolved oxygen measurements in the shallow emergent vegetation areas (zone 1) were consistently low, whereas dissolved oxygen concentrations in the water column near the hummocks (zone 4) were similar to concentrations in the emergent vegetation on the hummocks (Figure 7). Dissolved oxygen measurements at the surface and bottom of the open water near the hummocks (Figure 7b) demonstrate heterogeneities within the water column. Vertical mixing occurred during portions of the tracer test (i.e., 0–100 and 200–260 h) and thus support the use of a one-dimensional model in which concentration does not vary with depth. During other portions of the tracer test (100–200 h), stratification within the water column indicated weak vertical mixing and deviation from one-dimensional transport. Elevated dissolved oxygen concentrations near the surface suggest the presence of sheet flow and consequently tracer fronting.

[43] Additional simulations of breakthrough curves with significant fronting behavior (F03, F04) showed that transient storage provided a better fit with observed concentrations in the early parts of the experiment. In these cases, model simulations compensated for pronounced short-circuiting (tracer fronting) by invoking preferential flow in a main channel and secondary transport via transient storage (emergent vegetation and deep zones). This application of the transient storage model is contrary to traditional approaches that typically result in longer retention times and lower peak concentrations.

[44] The popularity of the one-dimensional modeling approach for investigating stream hydrodynamics is likely due to the overall simplicity of the combined field and modeling analysis. Tracer data are collected at a single well-mixed location and used to estimate transport parameters via nonlinear regression. Application of the one-dimensional modeling approach to wetland systems with high aspect ratios (length $\gg$ width) is a logical step beyond the conventional moment-based approaches but should proceed with caution due to inherent differences between wetland and stream systems. Aspect ratios in wetlands are typically lower than those of stream reaches, leading to a "near-field" problem in which traverse mixing is incomplete and application of the one-dimensional advection-dispersion equation is theoretically incorrect [*Rutherford*, 1994]. A second concern is the model's inability to reproduce polymodal tracer profiles (Figure 2) that are likely the result of multiple flow paths and short-circuiting. Given these concerns, more complex models that explicitly consider two-dimensional transport processes or multiple velocity profiles may be warranted. Although such models are available [*Werner and Kadlec*, 2000; *Lightbody et al.*, 2008; *Min and Wise*, 2009], the data requirements may exceed the resources and capabilities of most constructed wetland system operations. Use of one-dimensional models such as OTIS therefore represents a practical, albeit imperfect, approach that goes beyond the conventional moment-based analysis.

4. Conclusions

[45] After several years of operation, a surface flow wastewater treatment wetland near Phoenix, AZ, experienced a die-off of emergent vegetation resulting in decreased hydraulic performance. The 1.2 ha wetland was reconfigured to incorporate hummocks, and tracer experiments were conducted to evaluate hydraulic performance changes as the wetland matured from start-up conditions. The wetland underwent an acclimation period characterized by large cross-sectional flow areas. As the wetland matured, volumetric efficiencies were increasingly influenced by emergent vegetation. During the 4 year study period, the emergent vegetation was never fully established and total coverage was small. Therefore, small seasonal changes in vegetation spatial distribution had disproportionate effects on hydraulic properties. At the start of the growing seasons, transport was characterized by enhanced hydraulic performance. However, a distinct seasonal relation was established by the end of the growing seasons where lodged vegetation and short-circuiting characterized solute transport.

[46] Design elements such as hummocks ideally promote tortuous flow paths that effectively increase the aspect ratio of the wetland and reduce short-circuiting. However, the distribution of emergent vegetation also influences hydraulics and creates velocity heterogeneities (deviation from plug flow). Even so, the hummock-modified system had enhanced volumetric efficiencies as well as multiple secondary peaks on the breakthrough curves (similar to recirculation zones) suggesting the formation of both short and long flow paths by the hummocks. The polymodal nature of the tracer test results is reflective of the increased complexity of hydraulics in the hummock-modified system. On the basis of data presented here, as the wetland matures, a robust vegetation population over the hummocks and emergent zones of the

wetland will likely enhance mixing and increase hydraulic performance.

[47] **Acknowledgments.** This work was carried out with support from the U.S. Geological Survey National Research Program, Bureau of Reclamation, City of Phoenix, and Wass Gerke and Associates. The authors wish to thank Greg Brown, Jim Sartoris, Will Doyle, Joan Gable, Sara Gerke Lieske, Corey Perrella, Paul Kinshella, Wes Camfield, John Carlson, Kim Dannemiller, Charles Hart, Marnie Norris, R. Blaine McCleskey, and S. Mark Nelson for assistance. Use of trade names is for identification purposes only and does not constitute endorsement by the U.S. Geological Survey.

References

Atkinson, T. C., and P. M. Davis (2000), Longitudinal dispersion in natural channels: 1. Experimental results from the River Severn, *U.K. Hydrol. Earth Syst. Sci.*, *4*, 345–353.

Barber, L. B., J. A. Leenheer, T. I. Noyes, and E. A. Stiles (2001), Nature and transformation of dissolved organic matter in constructed wetlands, *Environ. Sci. Technol.*, *35*, 4805–4816.

Bastviken, S. K., S. E. B. Weisner, G. Thiere, J. M. Svensson, P. M. Ehde, and K. S. Tonderski (2009), Effects of vegetation and hydraulic load on seasonal nitrate removal in treatment wetlands, *Ecol. Eng.*, *35*, 946–952.

Bencala, K. E., and R. A. Walters (1983), Simulation of solute transport in a mountain pool-and-riffle stream: A transient storage model, *Water Resour. Res.*, *19*(3), 718–724, doi:10.1029/WR019i003p00718.

Burke, E. N., and B. W. Wadzuk (2009), The effect of field conditions on low Reynolds number flow in a wetland, *Water Res.*, *43*(2), 508–514.

Chapra, S. C. (1997), *Surface Water-Quality Modeling*, 844 pp., McGraw-Hill, Boston, Mass.

Chendorain, M., M. Yates, and F. Villegas (1998), The fate and transport of viruses through surface water constructed wetlands, *J. Environ. Qual.*, *27*, 1451–1458.

CH2M Hill (1997), Tres Rios Demonstration Constructed Wetland Project: Research Plan, report, Phoenix, Ariz.

Cronk, J. K., and M. S. Fennessy (2001), *Wetland Plants: Biology and Ecology*, 462 pp., A. F. Lewis, CRC Press, Boca Raton, Fla.

Danckwerts, P. V. (1953), Continuous flow systems: Distribution of residence times, *Chem. Eng. Sci.*, *2*, 1–13.

Daniels, J. S., B. S. Cade, and J. J. Sartoris (2010), Measuring bulrush culm relationships to estimate plant biomass within a southern California treatment wetland, *Wetlands*, *30*, 231–239.

Dierberg, F. E., and T. A. DeBusk (2005), An evaluation of two tracers in surface flow wetlands: Rhodamine-wt and lithium, *Wetlands*, *25*, 8–25.

Fogler, H. S. (1992), *Elements of Chemical Reaction Engineering*, 2nd ed., 838 pp., Prentice-Hall, Englewood Cliffs, NJ.

Hammer, D. A., and R. L. Knight (1994), Designing constructed wetlands for nitrogen removal, *Water Sci. Technol.*, *29*, 15–27.

Harvey, J. W., and B. J. Wagner (2000), Quantifying hydrologic interactions between streams and their subsurface hyporheic zones, in *Streams and Ground Waters*, edited by J. A. Jones, and P. J. Mulholland, pp. 3–44, Academic, San Diego.

Harvey, J. W., J. E. Saiers, and J. T. Newlin (2005), Solute transport and storage mechanisms in wetlands of the Everglades, South Florida, *Water Resour. Res.*, *41*, W05009, doi:10.1029/2004WR003507.

Headley, T. R., and R. H. Kadlec (2007), Conducting hydraulic tracer studies of constructed wetlands: A practical guide, *Ecohydrol. Hydrobiol.*, *7*, 269–282.

Hodgson, C. J., J. Perkins, and J. C. Labadz (2004), The use of microbial tracers to monitor seasonal variations in effluent retention in a constructed wetland, *Water Res.*, *38*, 3833–3844.

Jawitz, J. W. (2004), Moments of truncated continuous univariate distributions, *Adv. Water Resour.*, *27*, 269–281.

Jenkins, G. A., and M. Greenway (2005), The hydraulic efficiency of fringing versus banded vegetation in constructed wetlands, *Ecol. Eng.*, *25*, 61–72.

Kadlec, R. H. (1994), Detention and mixing in free water wetlands, *Ecol. Eng.*, *3*, 345–380.

Kadlec, R. H. (2003), Pond and wetland treatment, *Water Sci. Technol.*, *48*, 1–8.

Kadlec, R. H. (2007), Tracer and spike tests of constructed wetlands, *Ecohydrol. Hydrobiol.*, *7*, 283–295.

Kadlec, R. H. (2008), The effects of wetland vegetation and morphology on nitrogen processing, *Ecol. Eng.*, *33*, 126–141.

Kadlec, R. H. (2009), Wastewater treatment at the Houghton Lake wetland: Hydrology and water quality, *Ecol. Eng.*, *35*, 1287–1311.

Kadlec, R. H., and R. L. Knight (1996), *Treatment Wetlands*, 893 pp., CRC Press, Boca Raton, Fla.

Keefe, S. H., L. B. Barber, R. L. Runkel, and J. N. Ryan (2004a), Fate of volatile organic compounds in constructed wastewater treatment wetlands, *Environ. Sci. Technol.*, *38*, 2209–2216.

Keefe, S. H., L. B. Barber, R. L. Runkel, J. N. Ryan, D. M. McKnight, and R. D. Wass (2004b), Conservative and reactive solute transport in constructed wetlands, *Water Resour. Res.*, *40*, W01201, doi:10.1029/2003WR002130.

Knight, R. L., W. E. Walton, G. F. O'Meara, W. K. Reisen, and R. Wass (2003), Strategies for effective mosquito control in constructed treatment wetlands, *Ecol. Eng.*, *21*, 211–232.

Knowlton, M. F., C. Cuvellier, and J. R. Jones (2002), Initial performance of high capacity surface flow treatment wetland, *Wetlands*, *22*, 522–527.

Levenspiel, O. (1972), *Chemical Reaction Engineering*, 578 pp., John Wiley, New York, NY.

Lightbody, A. F., M. E. Avener, and H. M. Nepf (2008), Observations of short-circuiting flow paths within a free-surface wetland in Augusta, Georgia, U.S.A., *Limnol Oceanogr.*, *53*, 1040–1053.

Lightbody, A. F., H. M. Nepf, and J. S. Bays (2007), Mixing in deep zones within constructed treatment wetlands, *Ecol. Eng.*, *29*, 209–220.

Lin, A. Y.-C., J.-F. Debroux, J. A. Cunningham, and M. Reinhard (2003), Comparison of rhodamine WT and bromide in the determination of hydraulic characteristics of constructed wetlands, *Ecol. Eng.*, *20*, 75–88.

Martinez, C. J., and W. R. Wise (2003a), Hydraulic analysis of Orlando Easterly wetland, *J. Environ. Eng.*, *129*, 553–560.

Martinez, C. J., and W. R. Wise (2003b), Analysis of constructed treatment wetland hydraulics with the transient storage model OTIS, *Ecol. Eng.*, *20*, 211–222.

Min, J.-H., and W. R. Wise (2009), Simulating short-circuiting flow in a constructed wetland: The implications of bathymetry and vegetation effects, *Hydrol. Process.*, *23*, 830–841.

Nauman, E. B. (2008), Residence time theory, *Ind. Eng. Chem. Res.*, *47*, 3752–3766.

Nepf, H. M. (1999), Drag, turbulence, and diffusion in flow through emergent vegetation, *Water Resour. Res.*, *35*(2), 479–489, doi:10.1029/1998WR900069.

Oldham, C. E., and J. J. Sturman (2001), The effect of emergent vegetation on convective flushing in shallow wetlands: Scaling and experiments, *Limnol. Oceanogr.*, *46*, 1486–1493.

Persson, J. (2000), The hydraulic performance of ponds of various layouts, *Urban Water*, *2*, 243–250.

Persson, J. (2005), The use of design elements in wetlands, *Nordic Hydrol.*, *36*, 113–120.

Persson, J., N. L. G. Somes, and T. H. F. Wong (1999), Hydraulic efficiency of constructed wetlands and ponds, *Water Sci. Technol.*, *40*, 291–300.

Pfaff, J. D., D. P. Hautman, and D. J. Munch (1997), Method 300.1 Determination of inorganic anions in drinking water by ion chromatography, revision 1.0, *EPA/600/R98/188*, 40 pp., U. S. Environ. Protection Agency, Cincinnati, OH.

Runkel, R. L. (1998), One-dimensional transport with inflow and storage (OTIS): A solute transport model for streams and rivers, *Water Resour. Invest. Rep.*, *98-4018*, 73 pp., U.S. Geol. Surv., Denver, Colo.

Runkel, R. L., D. M. McKnight, and H. Rajaram (2003), Modeling hyporheic zone processes, *Adv. Water Resour.*, *26*, 901–905.

Rutherford, J. C. (1994), *River Mixing*, 347 pp., John Wiley, Chichester, England.

Sartoris, J. J., J. S. Thullen, L. B. Barber, and D. E. Salas (2000), Investigation of nitrogen transformations in a southern California constructed wastewater treatment wetland, *Ecol. Eng.*, *14*, p. 49–65.

Serra, T., H. J. S. Fernando, and R. V. Rodríguez (2004), Effects of emergent vegetation on lateral diffusion in wetlands, *Water Res.*, *38*, 139–147.

Somes, N. L. G., W. A. Bishop, and T. H. F. Wong (1999), Numerical simulation of wetland hydrodynamics, *Environ. Int.*, *25*, 773–779.

Stairs, D. B, and J. A. Moore (1994), Flow characteristics of constructed wetlands: Tracer studies of the hydraulic regime, in *Proceedings 4th International Conference on Wetland Systems for Water Pollution Control*, Guangzhou, China.

Stern, D. A., R. Khanbilvardi, J. C. Alair, and W. Richardson (2001), Description of flow through a natural wetland using tracer tests, *Ecol. Eng.*, *18*, 173–184.

Sun, X., and K. Shiono (2009), Flow resistance of one-line emergent vegetation along the floodplain edge of a compound open channel, *Adv. Water Resour.*, *32*, 430–438.

Thackston, E. L., F. D. Shields Jr., and P. R. Schroeder (1987), Residence time distribution of shallow basins, *J. Environ. Eng.*, *116*, 1319–1332.

Thullen, J. S., J. J. Sartoris, and W. E. Walton (2002), Effects of vegetation management in constructed wetland treatment cells on water quality and mosquito production, *Ecol. Eng.*, *18*, 441–457.

Thullen, J. S., J. J. Sartoris, and S. M. Nelson (2005), Managing vegetation in surface flow wastewater treatment wetlands for optimal treatment performance, *Ecol. Eng.*, *25*, 583–593.

Wagner, B. J., and J. W. Harvey (1997), Experimental design for estimating parameters of rate-limited mass transfer: Analysis of stream tracer studies, *Water Resour. Res.*, *33*, 1731–1741.

Wang, H., and J. W. Jawitz (2006), Hydraulic analysis of cell-network treatment wetlands, *J. Hydrol.*, *330*, 721–734.

Wang, H., J. W. Jawitz, J. R. White, C. J. Martinez, and M. D. Sees (2006) Rejuvenating the largest municipal treatment wetland in Florida, *Ecol. Eng.*, *26*, 132–146.

Wass, Gerke and Associates, Inc. (2001), Status report to the 1998 research plan for the Tres Rios demonstration constructed wetland project, report, 67 pp., Tempe, Ariz.

Wass, Gerke and Associates, Inc. (2007), Final Status Report (2005–2006 Study Period) Tres Rios Demonstration Constructed Wetlands, report, 59 pp., Tempe, Ariz.

Werner, T. M., and R. H. Kadlec (1996), Application of residence time distributions to stormwater treatment systems, *Ecol. Eng.*, *7*, 213–234.

Werner, T. M., and R. H. Kadlec (2000), Wetland residence time distribution modeling, *Ecol. Eng.*, *15*, 77–90.

Williams, C. F., and F. J. Adamsen (2008), A low-cost three-dimensional sample collection array to evaluate and monitor constructed wetlands, *Ecol. Eng.*, *33*, 83–90.

Wörman, A., and V. Kronnäs (2005), Effect of pond shape and vegetation heterogeneity on flow and treatment performance of constructed wetlands, *J. Hydrol.*, *301*, 123–138.

L. B. Barber and S. H. Keefe, U.S. Geological Survey, 3215 Marine St., Boulder, CO 80303, USA. (lbbarber@usgs.gov)

J. S. (Thullen) Daniels, U.S. Geological Survey, PO Box 25007, 86-68220, Denver, CO 80225, USA.

R. L. Runkel, U.S. Geological Survey, PO Box 25046, MS 415, Denver, CO 80225, USA.

E. A. Stiles, Bureau of Reclamation, PO Box 25007, Denver, CO 80225, USA.

R. D. Wass, Wass Gerke and Associates, Inc., 5010 E. Shea Blvd., Ste. A216, Scottsdale, AZ 85254, USA.